A Fast Method to Assess the Composition of a Polyolefin: An Application to Compliance Testing of Food Contact Materials

Guillaume Gillet,[1,2] Olivier Vitrac,[3] Stéphane Desobry[2]

[1]Centre Energie, Matériaux et Emballage, Laboratoire National de Métrologie et d'Essais, 78197 Trappes Cedex, France
[2]LSGA-ENSAIA-INPL, Nancy Université, 54505 Vandoeuvre lès Nancy, France
[3]UMR 1145 Génie Industriel Alimentaire, Institut National de la Recherche Agronomique, 91300 Massy, France

ABSTRACT: For plastics materials intended to be in contact with food, recent EU regulations, 72/2002/EC and 1935/2004/EC, enforce the assessment of the migration of 502 substances of the 932 positively listed substances. As mathematical modeling has been proposed to overcome such considerable effort in particular by providing maximum acceptable concentrations in the formulation, the compliance testing problem is efficiently reduced to the identification of substances and to their extent in initial materials. This work examines a fast identification and quantification procedure based on a semisupervised deconvolution procedure of FTIR spectra of polymer extracts in dichloromethane. The inversion procedure was implemented as a Tikhonov least-square problem and designed to work on large and open dictionary of substances by combining both spectra of reference additives and normalized responses of typical chemical functions. The sparsity of the overall solution was fulfilled with non-negativity constraints, while traces were detected by an iterative reweighting and stochastic resonance. The whole methodology was calibrated onto 21 typical additives of polyolefins and satisfactory tested on numerical examples and on extracts of processed films in high-density polyethylene including up to eight unknown compounds. Maps of possible confusions and biases were generated for all tested substances. The mass balance laws for molecules belonging to similar classes of additives were particularly highlighted. © 2010 Wiley Periodicals, Inc. J Appl Polym Sci 119: 1492–1515, 2011

Key words: FTIR; modeling; polyolefins; additives

INTRODUCTION

Along the food packaging chain, from raw materials up to finished products, the information and know-how is highly asymmetric between the different stakeholders: producers, converters, packaging fillers, retailers, enforcement laboratories, regulators, consumers, etc. The resulting incompleteness on a global market limits the usability of predictive mathematical models to check the compliance of materials and articles intended to come in contact with food or to assess their traceability to facilitate the control, the recall of defective products, consumer information, and the attribution of responsibilities, as encouraged by recent European regulations 2002/72[1] and 1935/2004.[2] In the case of thermoplastic materials used on the European market, the legislation, to which one of us participated, is particularly complex because it is both very detailed and it is still in the consolidation phase. Among the 937 substances (including 340 monomers and 597 additives), which are positively listed in EU directives on plastics in contact with food,[3] 502 substances (including 230 monomers and 272 additives) are thus subjected to specific migration limits (SMLs) because of toxicological concern. Substances, which are not authorized because they do not belong to the positive list, can also be used when they are located behind one or more layers, which prevents their migration into foods or food simulants above a detectable level.[4] This concept of relative barrier, so-called functional barrier, has been initially introduced to authorize the use of certain recycled materials for food contact applications. Although provisions are lacking or are divergent, this general principle tends today to be generalized to any multilayer structure and any substance including adhesives used in laminates, non-food contact material, and printing inks. In the context, where the EU Regulation 2023/2006[5] also lays down the responsibility of business operators, the development of rapid methods to identify possible migrants and their amount in the initial materials is

of significant concern. Indeed, each business operator should implement an effective quality management to select starting materials, which ensure compliance of the finished material or article. In absence of a certificate from the provider, which declares the compliance *a priori*, or for quality audit purposes, the extent of the migration of substances subjected to restrictions may be predicted via mathematical modeling, while avoiding unnecessary repetitions of time-consuming compliance studies. Modeling carried out in-house or outsourced has several benefits. It is an incremental procedure, which can handle several sources of uncertainty or variability (e.g., composition, geometry physicochemical properties, and storage conditions),[6] and, which can be used in real time to setup internal specifications: acceptable substances (e.g., molecular mass cutoff) and acceptable concentrations.[7]

The introduction of fingerprints in good manufacturing practices has been suggested in the early conclusions of the EU AIR research program CT94-1025,[8] but the recommended technique, [1]H-magnetic resonance, is still not widely available. Conventional deformulation techniques have been reviewed by Bart.[9] They involve mainly wet chemistry rules on material extracts, while combining an ever-increasing order of sophistication in analytical ingenuity. Previous studies demonstrated that the burden remained on the identification of substances and not on the extraction step itself, which can be optimized by an appropriate choice of solvent and an accurate estimate of the extraction yield.[10] For the fast discrimination of extracts involving volatile compounds, electronic noses based on metal oxide sensors have been proposed, but their applications are still restricted to the detection of off-odors and outgassing issues in thermoplastics.[9] FT-Raman spectroscopy combining with CCD array detectors and near-infrared diode laser excitation could be an appealing alternative to tag *in situ* additives according to their vibrational spectra.[11] However, the method is much less applied than infrared methods because of poor Raman scattering, insufficient reproducibility, and the lack of specific Raman libraries.[12] By contrast, mid-infrared spectroscopy is one of the most established analytical methods in the packaging industry and enforcement laboratories. In particular, Fourier transform infrared (FTIR) spectroscopy is supported by commercially available databases covering polymers and polymer additives, and it is suited for direct identification on either solid samples or extracts. Without being exhaustive, several studies[13–19] using mid-infrared techniques demonstrated the feasibility of the technique to trace the concentrations of minor constituents such as antioxidants in polyolefins. The usefulness of the technique to identify the formulation on commercial materials

(i.e., blind materials) including more than three additives and possible unknown components (i.e., without reference spectrum) has, however, never been tested. Unique identification and corresponding quantification in mixtures is expected to be hindered by the presence of similar functional bands regardless of the structure of the rest of the molecule.[20] Among foreseen difficulties, the spectra of large polymeric additives may be improperly assigned or the spectra of reactive phosphorous acid esters, used as hydroperoxide decomposers, may be confounded with very similar hindered phenolic antioxidants.[21] In the latter case, the confusion may have a significant impact on the safety of the tested material, as the SML is of 60 mg kg^{-1} for secondary antioxidants (hydroperoxide decomposers) against 6 mg kg^{-1} for primary antioxidants (hydrogen donors).[3]

Our objective was to design and discuss a general and robust framework to retrieve the identification and the quantification of major additives in commercial polyethylene materials by FTIR measurements for compliance testing purposes.[22] The originality of the approach was to include in the study the most used additives (21 additives) for packaging applications, while integrating complex mixtures combining an unknown number of additives and possibly nondocumented substances (not belonging to any positive list). It is underlined that handling unknown substances might help to prevent an accidental contamination of food products and subsequent crisis, such as the one generated by the contamination of baby milk[23] and other packaged drinks[24] by 2-isopropylthioxanthone. This article is organized as follows. Theory section describes the two-step semisupervised regression procedure, which was setup up for identification and quantification on mixtures including an unknown number of substances and possible unknown ones. The ill-posedness of the corresponding deconvolution problem prevented the use of common chemometrics techniques,[25] and it was minimized by introducing constraints on the solution such as non-negativity and sparsity. Resulting biases were decomposed and analyzed in terms of false positives and quantification biases. Experiments are described in Experimental section. As additives are heterogeneously distributed in the material, the methodology was applied to spectra of extracts in dichloromethane (DCM). This method was found to be more convenient for routine analysis as it avoids the scattering problem in semicrystalline polymers such as polyolefins. Results are presented in Results and Discussion section on either synthesized spectra or spectra of real extracts for four typical formulations of high-density polyethylene. Recommendations for compliance testing are summarized in Conclusions section.

THEORY

Forward problem: Decomposition of the spectrum of a mixture

For each measured wavenumber, λ, the FTIR absorption spectrum of a mixture (or an extract) in DCM, S_{tot}^{λ}, was interpreted as a linear superposition of the spectra due to DCM, S_{DCM}^{λ}, n additives $\{A_i\}_{i=1..n}$ belonging to a dictionary (i.e., database) of spectra, $\left\{S_{A_i}^{\lambda}\right\}_{i=1..n}$, m chemical groups $\{U_j\}_{j=1..n}$ not assigned to $\{A_i\}_{i=1..n}$, $\left\{S_{U_j}^{\lambda}\right\}_{i=1..n}$, extracted oligomers and other polymer residues (fillers, pigments, coatings…), S_{PM}^{λ}, and finally a normal error with zero mean ε^{λ}:

$$S_{\text{tot}}^{\lambda} = S_{\text{DCM}}^{\lambda} + \sum_{i=1}^{n} S_{A_i}^{\lambda} + S_{\text{PM}}^{\lambda} + \sum_{j=1}^{m} S_{U_j}^{\lambda} + \varepsilon^{\lambda}. \quad (1)$$

Except the spectrum of the background, all spectra were assumed to obey to the generalized Beer–Lambert law:

$$\begin{cases} S_{A_i}^{\lambda} = \alpha_{A_i}^{\lambda} C_{A_i} \\ S_{U_j}^{\lambda} = \alpha_{U_j}^{\lambda} \gamma_{U_j} \\ S_{\text{PM}}^{\lambda} = \alpha_{\text{PM}}^{\lambda} \gamma_{\text{PM}}, \end{cases} \quad (2)$$

where $\left\{\alpha_k^{\lambda}\right\}_{k=A_i, U_j, \text{PM}}$ are the products of molar extinction coefficient of the kth component at the wavenumber λ and the path length (i.e., the width of the cuvette which was a constant). $\{C_{A_i}\}_{i=..n}$, $\left\{\gamma_{U_j}\right\}_{j=1..m}$, γ_{PM} are the concentrations in A_i, U_i, and PM, respectively. By considering wavenumbers between 550 and 4000 cm^{-1} (3451 values), eqs. and lead to the following linear system:

$$\begin{bmatrix} S_{\text{tot}}^{\lambda_1} \\ S_{\text{tot}}^{\lambda_2} \\ ... \\ S_{\text{tot}}^{\lambda_{3451}} \end{bmatrix} = \begin{bmatrix} S_{\text{DCM}}^{\lambda_1} \\ S_{\text{DCM}}^{\lambda_2} \\ ... \\ S_{\text{DCM}}^{\lambda_{3451}} \end{bmatrix}$$

$$+ \begin{bmatrix} \alpha_{A_1}^{\lambda_1} & ... & \alpha_{A_n}^{\lambda_1} & \alpha_{U_1}^{\lambda_1} & ... & \alpha_{U_m}^{\lambda_1} & \alpha_{\text{PM}}^{\lambda_1} \\ \alpha_{A_1}^{\lambda_2} & ... & \alpha_{A_n}^{\lambda_2} & \alpha_{U_1}^{\lambda_2} & ... & \alpha_{U_m}^{\lambda_2} & \alpha_{\text{PM}}^{\lambda_2} \\ ... & ... & ... & ... & ... & ... & ... \\ \alpha_{A_1}^{\lambda_{3451}} & ... & \alpha_{A_n}^{\lambda_{3451}} & \alpha_{U_1}^{\lambda_{3441}} & ... & \alpha_{U_m}^{\lambda_{3451}} & \alpha_{\text{PM}}^{\lambda_{3451}} \end{bmatrix} \cdot \begin{bmatrix} C_{A_1} \\ ... \\ C_{A_n} \\ \gamma_{U_1} \\ ... \\ \gamma_{U_m} \\ \gamma_{\text{PM}} \end{bmatrix}$$

$$+ \begin{bmatrix} \varepsilon^{\lambda_1} \\ \varepsilon^{\lambda_2} \\ ... \\ \varepsilon^{\lambda_{3451}} \end{bmatrix},$$

which was written in a shorter form as:

$$\mathbf{S}_{\text{tot}} - \mathbf{S}_{\text{DCM}} = \mathbf{D}\mathbf{C} + \varepsilon. \quad (4)$$

A graphical interpretation is given in Figure 1 on a simple mixture. $\mathbf{S}_{\text{tot}} - \mathbf{S}_{\text{DCM}}$ is the spectrum associated to the mixture with the background associated to DCM subtracted. $\mathbf{D}$ is the dictionary matrix or calibration matrix containing the normalized spectra of all available substances and the spectra of functional groups associated to functional groups. As the measured intensity for a given chemical group depends on the sensitivity and linearity of the detector, an optimal $\mathbf{D}$ was obtained by generating the database on a same spectrometer instead of using a commercial database. An additional interest was to take into account possible interactions with DCM and to weight wavelengths according to the linearity of the detector. A realistic solution $\mathbf{C}$ must minimize the L^2-norm $\|\varepsilon\|^2$ (variance of ε) while ensuring ε has a zero mean. As the number of wavenumbers is much greater than the number of unknown compounds, the linear system was extensively overdetermined. To avoid additional confusion between the bands present in documented additives (i.e., in A_i) with generic bands (i.e., in U_j), generic bands were associated to bump functions, which guaranteed smooth cutoffs [see Fig. 1(a)].

Equation was relaxed to optimal wavelengths by introducing a weighting 3451 × 3451 diagonal matrix, $\mathbf{W}$, whose main diagonal elements were ranged between 0 and 1:

$$\underbrace{\mathbf{W}(\mathbf{S}_{\text{tot}} - \mathbf{S}_{\text{DCM}})}_{\Sigma} = \underbrace{\mathbf{W}\mathbf{D}}_{\Delta} \mathbf{C} + \mathbf{W}\varepsilon. \quad (5)$$

The relative weight of each wavenumber was determined from the determination coefficient, $\left\{r_{\lambda,i}^2\right\}_{i=1..n}$, derived from the calibration curve of binary mixtures DCM + A_i obtained for five different concentrations. As a heuristic (semisupervised regression), a weight of 1 at λ was assigned when one of the three following properties was fulfilled:

1. All $\left\{r_{\lambda,i}^2\right\}_{i=1..n}$ values were greater than 0.7 with at least one value above 0.9;
2. At least one $\left\{\alpha_{A_i}^{\lambda}\right\}_{i=1..n}$ was higher than the 70th percentile values of the whole spectrum $\left\{\alpha_{A_i}^{\lambda}\right\}_{\lambda=\lambda_1..\lambda_{3541}}$;
3. At least one $\left\{\alpha_{U_j}^{\lambda}\right\}_{j=1..m}$ is significantly higher than 1.

To increase the signal-to-noise ratio, a smooth spline cutoff was applied to adjacent wavenumbers with a cutoff of 5 cm^{-1} and a transition width of 3 cm^{-1}. It was verified that this low-cost procedure was almost
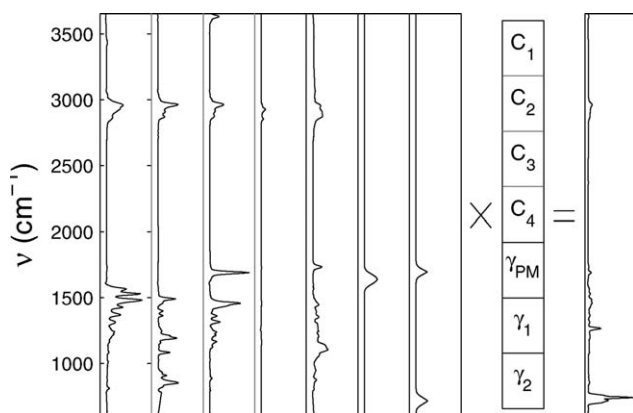
Figure 1 Graphical interpretation of normal equation (5), $\Sigma = \Delta C$, for a mixture including Irganox 1076 (concentration C_1), Irgafos 168 (concentration C_2), erucamide (concentration C_3), and Chimassorb 944 (concentration C_4) in polyethylene (concentration γ_{PM}). γ_1 and γ_2 stand for the concentrations in simple chemical functions (respectively), whose normalized spectra are plotted in columns 6 and 7 of Δ.

equivalent to a filtering step with zero-phase low pass band filter of bandwidth 10 cm^{-1}. At the end, for the 21 considered additives and 15 additional chemical groups, 354 wavenumbers had a weight equal to 1.

The contribution of the polymer was obtained similarly from the calibration curve obtained for five different virgin polymer extracts. Because the substances were unknown, $\left\{\gamma_{U_j}\right\}_{j=1..m}$ and γ_{PM} were expressed in arbitrary units.

Inversion problem: Finding concentrations of unknown compounds

Linear system, written as $\Sigma = \Delta C$, was poorly conditioned because of significant correlations between the FTIR spectra of additives with close chemical formula or including repeated patterns. The practical consequence was that the large null space of $\underline{B}$ dominated the solution vector, C, of the standard least-square problem $C = \arg\min\|\Sigma - \Delta C\|^2$. Indeed, any vector of the null space, ΔC, could be added to calculate a new solution of $\Sigma = \Delta C$. Without correction, this method would give concentration estimates highly sensitive to noise measurements as well as numerous false positives and erroneous quantifications. To reduce such artifacts, a ridge regression was used instead and implemented as the following Tikhonov regularization problem[26]:

$$C = \arg\min\|\Delta C - \Sigma\|^2 + \xi^2\|\Delta_\Gamma C\|^2$$

$$= \arg\min\left\|\begin{bmatrix} \Delta \\ \xi\Delta_\Gamma \end{bmatrix} C - \begin{bmatrix} \Sigma \\ 0 \end{bmatrix}\right\|^2$$

$$\text{subjected to } \{C_i \geq 0\}_{i=1...n+m+1}, \quad (6)$$

where Δ_G is a $(n + m + 1) \times (n + m + 1)$ diagonal matrix, where the diagonal term is zero when the con-

centration component is not subjected to any restriction (it may be present) and 1 otherwise, when its content is expected to be minimal or zero. In other words, the sparsity of the solution for unknown compounds $\{U_j\}_{j=1..m}$ (i.e., minimizing false positives) was enforced by introducing an additional distance constraint, $\xi^2\|\Delta_\Gamma C\|^2$. The tradeoff between the minimization of the fitting error and the constraint was controlled by a positive constant ξ, so-called Tikhonov constant. As recommended by Hansen,[27] ξ was set to homogenize variances between measurements and predictions:

$$\xi^2 = \frac{\text{var}(S_{tot} - S_{DCM}, \text{diag}(W))}{\text{var}(C, \text{diag}(I))}, \quad (7)$$

where var(u,v) is the variance of vector u relatively to the vector of weights v, diag(W) is the main diagonal of W, and I is the identity matrix.

As C is not known *a priori*, an iterative procedure is applied by starting with $\xi = 0$ (unregularized problem) in eq. . Under these assumptions, the calculated solution is the most likely according to available measurements and the available database. In addition, positivity constraints in eq. restricted all solutions only to feasible ones. They were efficiently handled using an iterative inversion procedure method based on the interior-reflective Newton method.[28] The method was started from the solution calculated without constraint from the truncated singular value decomposition of $[\Delta \quad \xi\Delta_\Gamma]^T$.

The whole strategy prevented noise components in the null space (due to mainly overlapping regions in spectra) to propagate significantly in the approximated concentration vector. However, the presence of unexplained residues in the measured spectrum increased the risk of overestimation of identified compounds. When disambiguation needed to be verified or when quantification should be improved because of nonassigned residual bands in $W\varepsilon$, $W_{\lambda\lambda}$ components with nonzero values were replaced by $1/|\varepsilon_\lambda|$. Although the convergence was not guaranteed, such refinements focused on measured spectrum components, for which the variance could be the best explained. This reweighting strategy guaranteed that the whole methodology would be applied to any mixture and polymer sample even when some peaks or patterns could not be recognized.

Biases associated to identification and quantification

Difficulties in assessing the composition of even simple mixtures are illustrated in Figure 2. In this theoretical example, an additive with a two-band
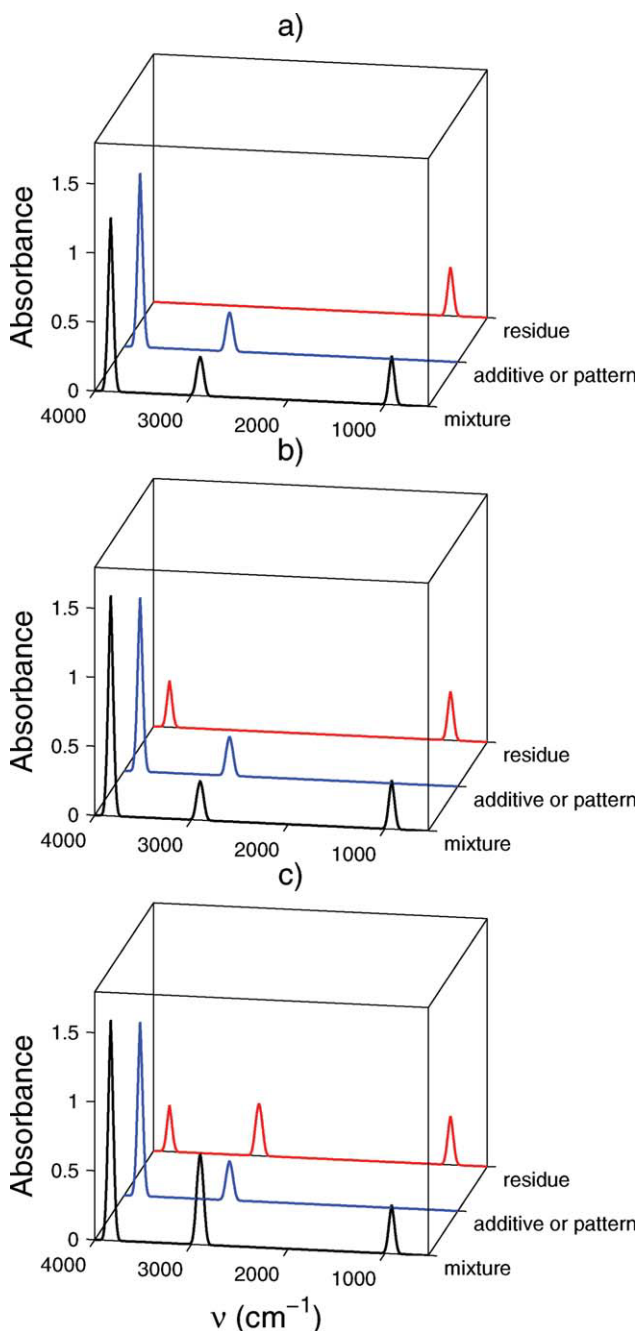
Figure 2 Theoretical example including an additive with a known spectrum (including three bands) and an unknown substance or residue with: (a) no common band, (b) one common band, and (c) two common bands. [Color figure can be viewed in the online issue, which is available at wileyonlinelibrary.com.]

spectrum was mixed with an unknown substance including, according to the considered scenario: no common band [Fig. 2(a)], one common band [Fig. 2(a)], and two common bands [Fig. 2(c)]. The objective was to retrieve the true concentration of the additive (here three in arbitrary units), C_A, when only the spectra of the mixture, Σ, and of the additive, S_A, were known. The ratio between the known and

unknown substances was set to 2/3. In this simple example, the Moore-Penrose pseudoinverse was $0.1252 S_A^T$, and the solution corresponding to the theoretical normal equation, $\Sigma = S_A C_A$, was $0.1252 SS_A^T \Sigma$. This crude approach, which neglected the unknown substance, led to C_A values equal to 3, 3.75, and 4.02 when no, one, and two common bands were present. Because adding 20% white noise to S_A and Σ gave 2.92, 3.74, and 3.97, respectively, the C_A estimates were almost insensitive to noise, but results were biased when a nonindexed substance was present. The overestimation observed, when at least one common band was present, was caused by the indiscernibility of the response for some wavenumbers. As previously suggested, increasing the weight of wavenumbers where the predicted spectrum was underestimated could help to reduce the bias. In the absence of noise, the corrected estimates were 3, 3, and 3.8, respectively. In the presence of noise, the correction was much less efficient because of significant confidence intervals on predictions, which hindered the identification of the spectrum regions, where the predictions overestimated the measures. On real samples, bands that looked homothetic exhibited subtle differences, which were expected to increase the well posedness of the mathematical attribution of bands.

The biases associated to an erroneous attribution of bands were calculated systematically by analyzing all the 21×20 binary mixtures (note that the matrix of pair interactions is symmetric), mixing a substance X and a substance Y with $X \neq Y$. The overall objective was to retrieve a table of possible pairs, which might yield a false identification of the substance, a poor detection level, an erroneous quantification, etc. when the whole dictionary of known substances (21) was used for the identification. For a given pair, the total bias, β_{tot}, was decomposed as:

$$\beta_{tot} = \left\langle \hat{C}_Y^{all} - C_Y \right\rangle_Y = \beta_{00} + \left\langle \beta_{X0}^{XY} \right\rangle_X + \left\langle \beta_{X0}^{all} \right\rangle_X$$
$$+ \left\langle \beta_{X0}^{XY} \right\rangle_Y + \left\langle \beta_{X0}^{all} \right\rangle_Y + \left\langle \beta_{0Y} \right\rangle_Y + \left\langle \beta_{XY}^{XY} \right\rangle_{X,Y} + \left\langle \beta_{XY}^{all} \right\rangle_{X,Y} \quad (8)$$

where $\hat{C}_Y^{all}$ is the estimated concentration in Y when the whole inversion procedure was applied, C_Y is the "true" concentration in Y in the mixture. For each pair X and Y, a normalized range of concentrations including 11 levels for C_X and C_Y (11×11 combinations) was used to evaluate biases. To get realistic estimates, a 10% white noise was added to the spectrum of each mixture. $\langle\rangle_L$ is the average operator over all realizations, which verifies the subset of rules L.

β_{00} is the systematic bias due to identification irrespectively of the considered substances. $\left\langle \beta_{X0}^{XY} \right\rangle_X$ and $\left\langle \beta_{X0}^{all} \right\rangle_X$ assess the nonspecific false detection level associated to the substance X when no other substance is added to the mixture, respectively, when

the dictionary is reduced to substances X and Y, and when all known substances are incorporated. $\langle \beta_{X0}^{XY} \rangle_Y$ and $\langle \beta_{X0}^{all} \rangle_Y$ assess the false detection level on Y related to the incorporation of any substance X, respectively, when the dictionary is reduced to substances X and Y, and when all known substances are incorporated.

$\langle \beta_{0Y} \rangle_Y$ is the bias of quantification associated to Y alone, when no other substance is added to the mixture. This bias was different of 0 only when the whole dictionary was used. $\langle \beta_{XY}^{XY} \rangle_Y$ and $\langle \beta_{XY}^{all} \rangle_Y$ assess the biases-associated interaction between X and Y, respectively, when the dictionary is reduced to substances X and Y, and when all known substances are incorporated.

EXPERIMENTAL

Formulation of samples

To test the whole identification and quantification methodology on real samples, four high-density polyethylenes with typical formulations were formulated at semi-industrial scale. Formulations are detailed in Table I, and they include antioxidants, light stabilizers, surface agents, and swelling agent. Chemical structures of additives are represented in Table I. They include most of typical chemical groups absorbing in FTIR: alcohol, aldehyde, ketone, aromatic circle, *tert*-butyl, ester, thioester, phosphite, amine, amide, benzotriazine, and benzotriazol. Plastic additives were provided by Ciba (Switzerland) except Erucamide, which was obtained from Croda (Italy), and calcium stearate, which was obtained from Merck (Germany). Virgin high-density polyethylene was obtained from ATOCHEM (France). Polymer flakes were formulated during a first extrusion step before final processing at semi-industrial scale as 150-mm-wide and 0.2-mm-thick ribbons by a second extrusion and subsequent calendering. Both extrusion steps were performed at 200°C, and polymer flakes were dried during 4 h at 40°C between formulation and final processing. The final density and the melting point were of 940 kg m^{-3} and 136°C, respectively. The crystallinity was evaluated to 72.5% by differential scanning calorimetry.

Extraction of additives from samples

Extraction of additives from films was performed by soxhlet extraction in DCM (ACROS organics, Belgium). Ten grams of films cut in 5 mm × 5 mm pieces were placed in contact with 100 mL of DCM, 40 h, at 40°C. To prevent the degradation of additives and polymer chain scissions during the extraction step, 100 μL L^{-1} of triethylphosphite (Sigma-Aldrich, USA) was added to DCM. Long-term extraction was required to get accurate reference estimates of the formulation of processed films. For compliance testing or rapid screening, this constraining procedure could be replaced by a 40-min pressurized solid–liquid extraction.

Reference concentration measurements

Reference concentrations were measured by high-performance liquid chromatography (HPLC) associated to an UV diode array detector and an evaporative light scattering detector in series. The HPLC protocol was similar to the one described by Garrido-López and Tena.[29] The HPLC system consisted of a Waters 717plus autosampler, a Waters 600 controller equipped with a thermostatted column compartment, and an in-line degasser AF (Waters, USA). Separation was achieved on an Xterra C8 column (150 mm × 3.0 mm; 5-μm particles; Waters, USA) operated at 60°C.

FTIR measurements

Absorption spectra of extracts in DCM were acquired between 4000 and 550 cm^{-1} in a 100-μm-thick cuvette (model moni-cell, Eurolab, Germany) located in a Fast FTIR spectrometer (model spectrum One, Perkin-Elmer, USA) at 23°C. Reference spectra of additives at different concentrations, ranging between 10^{-1} and 10^{-4} mol L^{-1}, were acquired similarly in DCM.

As previously discussed, to increase the sensitivity to small differences, a white noise, ranged between 0.1 and 1%, and smaller than the repetition error, was added to measured spectra before applying the deconvolution. This procedure was repeated until to achieve a convergence of concentration estimates.

RESULTS AND DISCUSSION

FTIR spectra of a typical BHT pattern

Absorption spectra of a typical additive pattern, BHT, are plotted in Figure 3 when the contribution of the solvent DCM was removed. The linear increase of the band absorption with concentration was used to identify specific mid-infrared bands of BHT. The proposed assignation of bands relied on the analysis proposed in Ref. [30]. The fundamental vibrations in the 3700–3600 cm^{-1} region were due to O—H stretching of the phenol group. The broad band between 3100 and 3000 cm^{-1} was associated to C—H attached to the aromatic ring. The 1500–650 cm^{-1} region with a forest of bands was referred as the finger print region, which revealed the signature of most bending and skeletal vibrations. It is worth

TABLE I
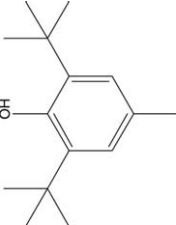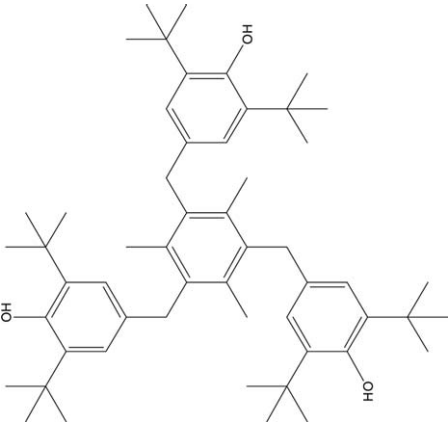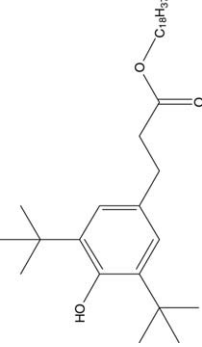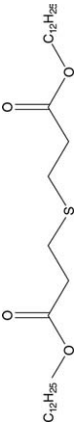**Substances Tested and Listed in the Dictionary for Identification and Quantification**

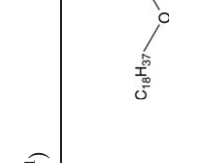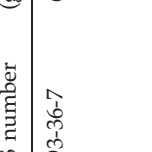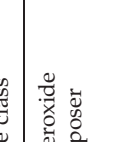| Distance rank[a]	Commercial name	Systematic chemical name	Additive class	CAS number	M (g mol^{-1})	Chemical structure
1	BHT	2,6-Di-*tert*-butyl-4-methylphenol	Hydrogen donor	000128-37-0	220	
2	Irganox 1330	1,3,5-Trimethyl-2,4,6-tris(3,5-di-*tert*-butyl-4-hydroxybenzyl)benzene	Hydrogen donor	01709-70-2	774	
3	Irganox 1076	Octadecyl 3-(3,5-di-*tert*-butyl-4-hydroxyphenyl) propionate	Hydrogen donor	2082-79-3	530	
4	Irganox PS800	Thiodipropionic acid, didodecyl ester	Hydroperoxide decomposer	00123-28-4	515	

TABLE I. *Continued*
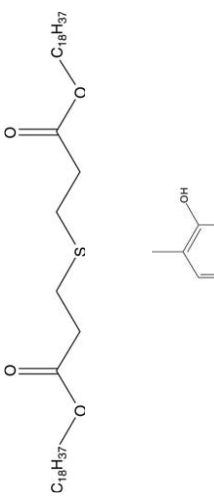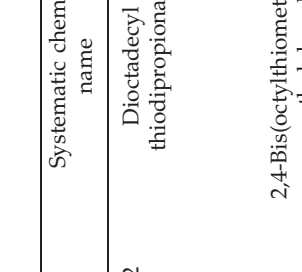
Distance rank[a]	Commercial name	Systematic chemical name	Additive class	CAS number	M (g mol^{-1})	Chemical structure
5	Irganox PS802	Dioctadecyl thiodipropionate	Hydroperoxide decomposer	00693-36-7	683	
6	Irganox 1520	2,4-Bis(octylthiomethyl)-6-methylphenol	Multifunctional hydrogen donor	110553-27-0	424	
7	Atmer 163	N,N-bis(2-hydroxyethyl)-alkyl(C13-C15)amine	Antistatic agent	107043-84-5	287–315	
8	Stearic acid	Octadecanoic acid	Lubricant	00057-11-4	268	
9	Erucamide	(13Z)-docos-13-enamide	Slip agent	00112-84-5	337	
10	Tinuvin 326	2-(2-Hydroxy-3-*tert*-butyl-5-methylphenyl)-5-chlorobenzotriazole	UV absorber	03896-11-5	316	

TABLE I. *Continued*

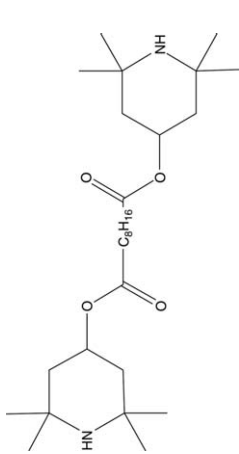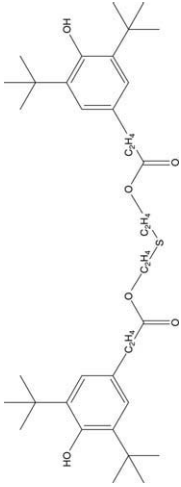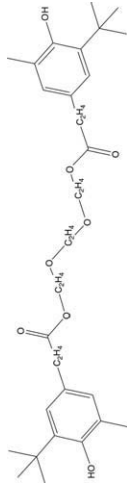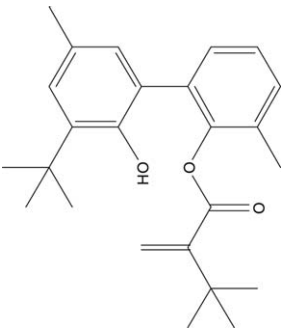| Distance rank[a]	Commercial name	Systematic chemical name	CAS number	M (g mol^{-1})	Additive class	Chemical structure
11	Tinuvin 770	Bis(2,2,6,6-tetramethylpiperidin-4-yl) decanedioate	52829-07-9-	481	Radical scavenger	
12	Irganox 1035	Thiodiethanol bis(3-(3,5-di-*tert*-butyl-4-hydroxyphenyl) propionate)	41484-35-9	642	Multifunctional hydrogen donor	
13	Irganox 245	Triethyleneglycol bis(3-(3-*tert*-butyl-4-hydroxy-5-methylphenyl) propionate)	036443-68-2	586	Hydrogen donor	
14	Irganox 3052	2-(1,1-Dimethylethyl)-6-[3-(1,1-dimethylethyl)-2-hydroxy-5-methylphenyl] methylphenyl acrylate	61167-58-6	394	Multifunctional hydrogen donor	
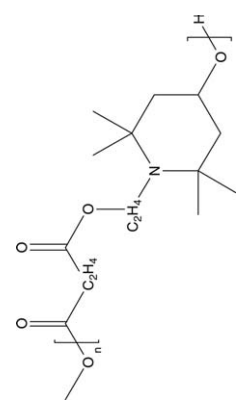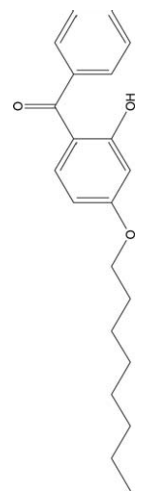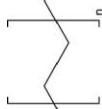
TABLE I. *Continued*

Distance rank[a]	Commercial name	Systematic chemical name	Additive class	CAS number	M (g mol^{-1})	Chemical structure
15	Tinuvin 622	Poly(4-hydroxy-2,2,6,6-tetramethyl-1-piperidine ethanol-alt-1,4-butanedioic acid)	Light stabilizer	65447-77-0	3100–4000	
16	Irgafos 168	Tris(2,4-di-*tert*-butylphenyl) phosphite	Hydroperoxide decomposer	31570-04-4	647	
17	Chimassorb 81	2-Hydroxy-4-*n*-octyloxybenzophenone	Light stabilizer	01843-05-6	326	

TABLE I. *Continued*

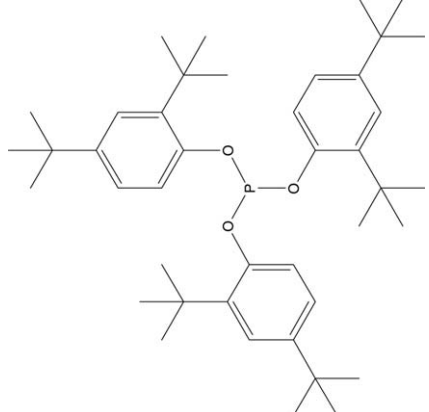| Distance rank[a]	Commercial name	Systematic chemical name	CAS number	M (g mol^{-1})	Chemical structure
18	Chimassorb 944	Poly[6-[(1,1,3,3-tetramethylbutyl)amino]-1,3,5-triazine-2,4-diyl]-[(2,2,6,6-tetramethyl-4-piperidyl)-imino]hexamethylene[(2,2,6,6-tetramethyl-4-piperidyl)imino]	71878-19-8	2000–3100	
19	Irganox 3114	1,3,5-Tris(3,5-di-*tert*-butyl-4-hydroxybenzyl)-1,3,5-triazine-2,4,6(1H,3H,5H-)trione	27676-62-6	784	
20	Irganox 1010	Pentaerythritol tetrakis(3-(3,5-di-*tert*-butyl-4-hydroxyphenyl)propionate)	06683-19-8	1178	

TABLE I. *Continued*

Distance rank[a]	Commercial name	Systematic chemical name	Additive class	CAS number	M (g mol^{-1})	Chemical structure
21	Triethylphosphite	Triethylphosphite	Hydroperoxide decomposer	122-52-1	166	
22	PE	Polyethylene	—	—	$16n + 2$	

[a] Rank corresponding to the Euclidian distance between normalized spectra as depicted in Figure 5(b).

to notice that the vibrational response of DCM perturbed some bands in this region, so that the subtracted spectra appeared discontinuous at some wavenumbers [Fig. 3(a)].

Our automatic weighting procedure recognized accordingly the major bands and in particular the signature of the random reorientation of both *tert*-butyl groups. By combining the information of all tested 21 additives (Table I), it was obvious that most of the available degrees of freedom for identification came from the fingerprint region and were controlled by the lateral hindering groups. Indeed, the alcohol band and the rigid C—H bands were much less specific as most of antioxidants included a phenol group. Only the terminal part of the 1830–1650 cm^{-1} region of carbonyl group was incorporated in the full analysis. Secondary amine groups stretching, usually observed between 3400 and 3300 cm^{-1}, was also selected for Atmer, Chimassorb 944, and Tinuvin series. Aromatic C—N stretching in triazine and in aromatic amines, the aliphatic C—N stretching, and the N—H wagging band were also included, respectively, at 1590–1520 cm^{-1}, 1360–1250 cm^{-1}, 1220–1020 cm^{-1}, and around 715 cm^{-1}. The aliphatic P—O stretching and the thioether function, present in secondary antioxidants, were merged in the middle of the finger print region at 1450–1430 cm^{-1} and at 700–600 cm^{-1}, respectively. Finally, C—H stretching bands from aliphatic domains, which occur in the range 3000–2850 cm^{-1}, were also introduced to derive the contribution of oligomers in the mixture.

Degrees of similitude between the FTIR spectra of tested additives

The presence of resembling chemical groups for molecules with similar technological function complicated the identification of those substances. This effect is illustrated in Figure 4 by comparing the normalized spectra of additives, Irganox 1076 and Irganox PS800, with partly dissimilar chemical structures but with close signatures. The concentration ratio, which maximized the resemblance between the spectra of both additives, was determined from the right-singular vectors of Δ reduced to the two additives columns. The C—H stretching band from aliphatic segments in the range 3000–2850 cm^{-1} dominated the response of both molecules. The carbonyl stretching in the 1830–1650 cm^{-1} region was highly recognizable but not enough specific to separate both molecules. Tenuous differences appeared along the whole fingerprint region. Although they contributed to about 21% of the overall mean square difference between both spectra, they were much more specific.
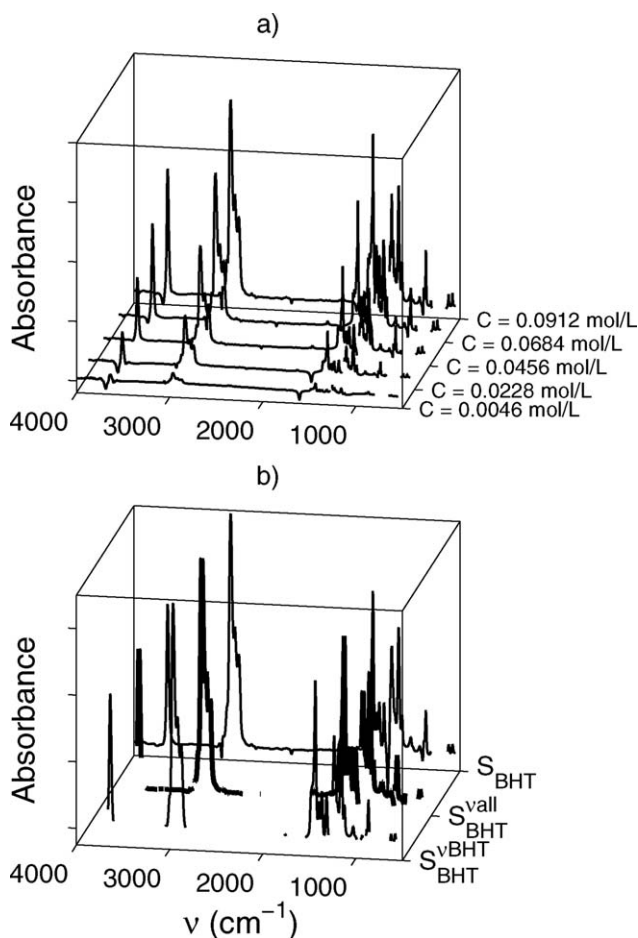
Figure 3 Absorption FTIR spectra of BHT in DCM with background subtracted: (a) raw spectra at different concentrations, (b) spectra regions with a relative weight of 1 according to the number of additives considered in the dictionary: BHT alone (S_{BHT}^{vBHT}) and BHT with the full database (S_{BHT}^{vall}).

To assess the importance of the fingerprint region in the separation of substances, the former comparison was applied to all 22 × 22 pairs including the 21 additives and the polymer itself. The Euclidian distances between all spectra, assembled as a similarity matrix, were used to reconstruct a theoretical map of proximities between tested substances in a low-dimensional space. The scatter was maximized by projecting the distances onto a three-dimensional space with an average distance error of 16% and a maximum error up to 60%. The same similarity matrix was used to obtain a hierarchical classification of the proximity of spectra based on the averaged distances between groups of substances. Distance maps and dendrograms are plotted in Figure 5 when the whole spectra or the fingerprint regions were used. They confirmed that only few substances could be identified undoubtedly, among them: Tinuvin 622, Irganox 1010, Triethylphosphite, and Chimassorb 944. The analysis of the fingerprint region increased glob-

ally the discrimination, with significant improvements for Irgafos 168 and Chimassorb 81. On one hand, the small distances generally observed between spectra confirmed the mathematical ill-posedness of the inversion of eq. (6). On the other hand, the distances maps suggested that clustering of molecules, whose distances were below a threshold normalized distance (e.g., 0.5), could help to identify the number of some typical chemical patterns present in the mixture. Thus, although BHT, Irganox 1330, Irganox 1035, and Irganox 1076 had very similar spectra, the concentration in BHT patterns could be guessed from their responses in the fingerprint region as they were almost proportional to the number of embedded BHT, respectively, 1, 4, 2, and 1.

Biases estimates on binary mixtures

Previous considerations were based on well-defined spectra of molar extinction coefficients and not on crude spectra of mixtures. In addition, they did not take into account and the cutoff distance introduced by the inversion procedure itself. Biases associated to the similarities among the 21 additives were calculated by applying the whole procedure to all combinations of binary mixtures. A white noise level of 5% was added to all mixtures, and the concentrations were sampled from 500 repetitions. The biases
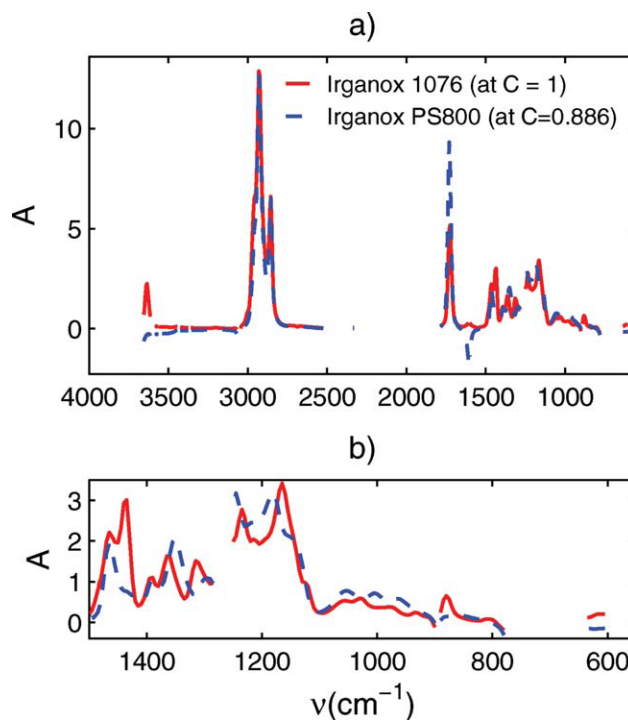

Figure 4 Spectra of Irganox 1076 and Irganox PS800 normalized to maximize similitudes: (a) whole range of wavenumbers and (b) details in the fingerprint region. [Color figure can be viewed in the online issue, which is available at wileyonlinelibrary.com.]
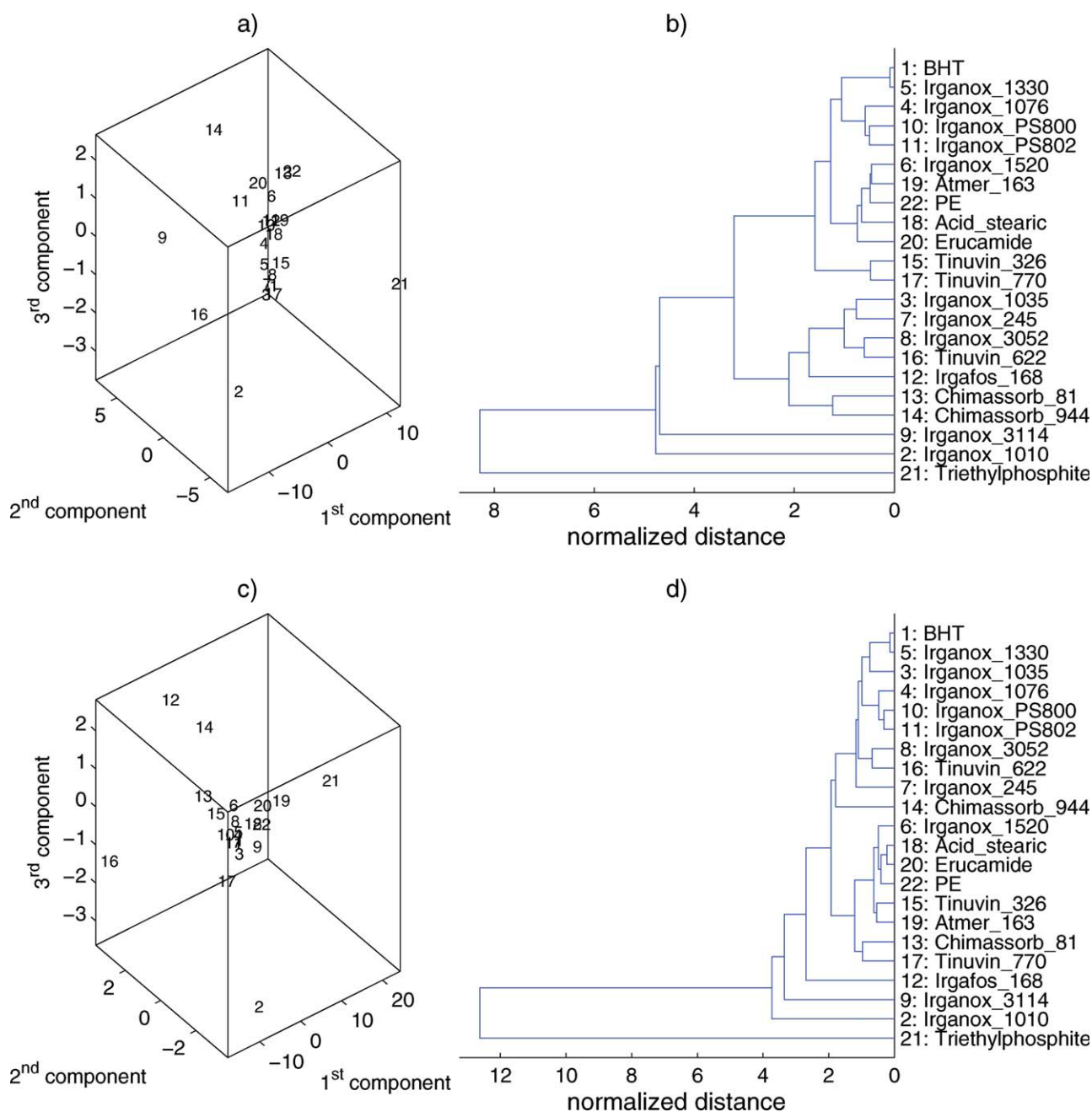
Figure 5 Distance map between spectra of tested substances: (a, b) whole spectra and (c, d) fingerprint region. [Color figure can be viewed in the online issue, which is available at wileyonlinelibrary.com.]

were linearly decomposed according to eq. (8). To assess the relevance of non-negativity constraints, detection biases were calculated according to unconstrained solutions of eq. (6). The systematic bias, β_{00}, was found not significant. The other biases, related to identification and to quantification, are summarized in Figures 6 and 7, respectively, for a dictionary including only the two tested molecules or the whole set of 21 additives. All molecules were indexed according to the overall distances between spectra plotted in dendrogram 6b to highlight the correlations between biases and spectra closeness.

The disruptor character of a given substance in a mixture was assessed by a $\left\langle \beta_{X0}^{XY} \right\rangle_X$ or $\left\langle \beta_{X0}^{all} \right\rangle_X$ value different from 0 [Fig. 6(a,b)]. Only Tinuvin 326, an ultraviolet absorber, including amines functions and a BHT pattern, acted as a "chimera" and hindered the detection of several substances with partial resemblance. Its signature was, however, unique and it was always detected, when it was present. Molecules subjected to an elevated risk of false positive were revealed by a significant positive bias $\left\langle \beta_{X0}^{XY} \right\rangle_Y$ or $\left\langle \beta_{X0}^{all} \right\rangle_Y$ [Figs. 6(c) and 7(d)]. On the opposite, molecules with high detection threshold were identified
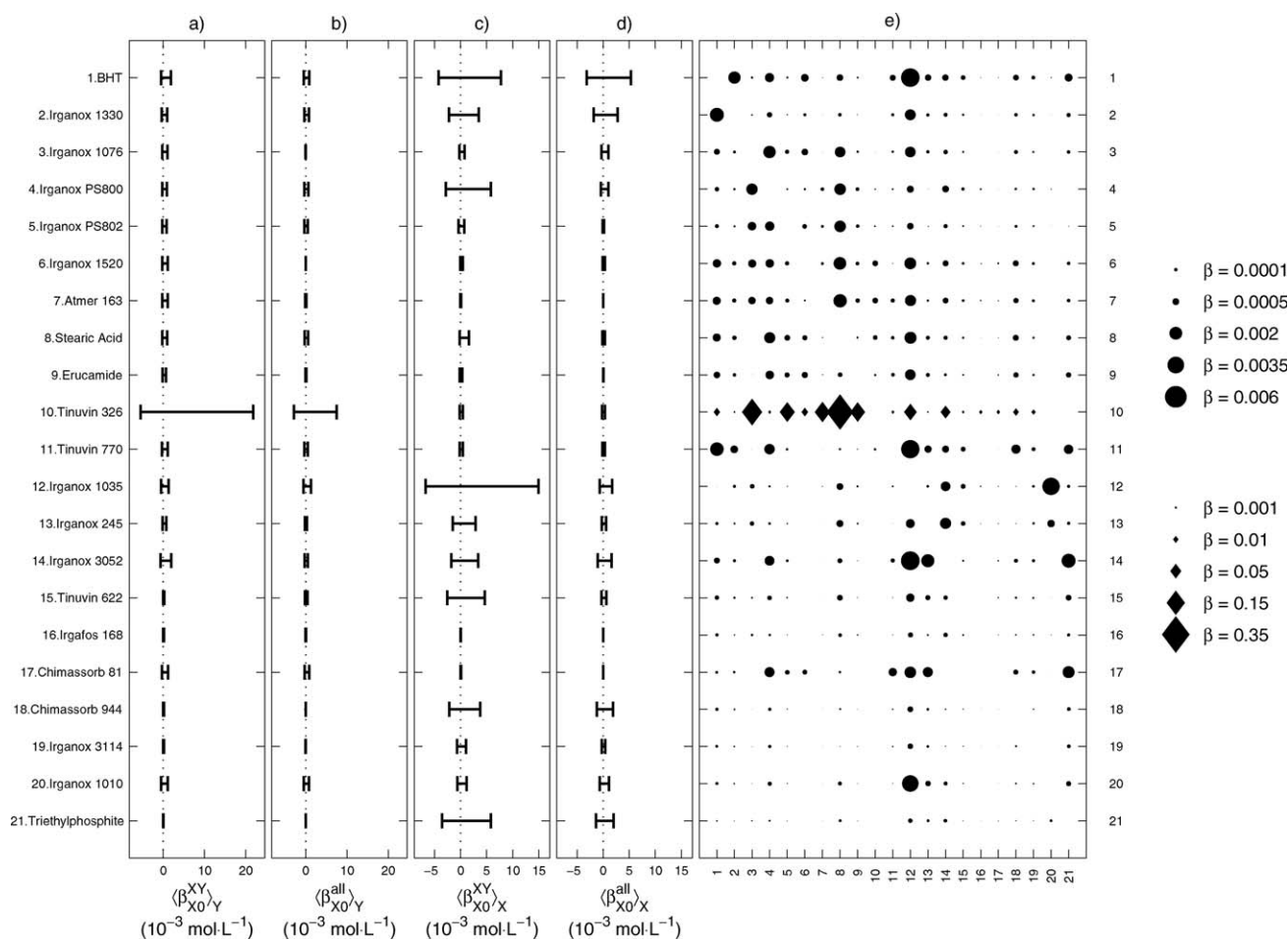
Figure 6 Identification biases on Y for binary mixtures $X + Y$ as defined in eq. (8) when Y is not present in the mixture: (a, b) average false detection level generated by all substances X listed in the dictionary, $\left\langle \beta_{X0}^{XY} \right\rangle_Y$ and $\left\langle \beta_{X0}^{all} \right\rangle_Y$; (c, d) average false detection levels generated by the substance X on all possible Y listed in the dictionary, $\left\langle \beta_{X0}^{XY} \right\rangle_X$ and $\left\langle \beta_{X0}^{all} \right\rangle_X$; (e) false detection associated to a specific substance X. Biases in a and c were calculated with dictionaries containing only molecules X and Y, whereas they were calculated with all 21 additives in b, d, and e. Signed biases were obtained by removing non-negativity constraints in eq. (6). Substances are ordered according to the distances between spectra plotted in Figure 5(b).

by a negative bias. Working with a large set of substances in the database reduced both risks by spreading the total variance on more degrees of freedom (i.e., more substances). The confusion matrix [Fig. 6(e)] revealed that all substances including a significant pattern such as BHT or several amine functions were subjected to significant detection threshold, as they might be replaced by molecules with a similar pattern. In practice, large spots in the confusion matrix read column-wise should be interpreted as falsely detected molecules susceptible to mask the one indicated on the row title. The masking intensity was expressed as the expected molar concentration in the true substance. Reciprocally, the same matrix read row-wise gave the underestimation factor because of a false assignment to other substances.

Quantification biases took into account the interactions between pairs of additives. As these interactions were associated to confusion between substances, they were mainly negative. The true concentrations were on an average lowered by a value $\langle \beta_{0Y} \rangle_Y$ when only the measured substance was present in the mixture [Fig. 7(a)]. As expected from previous behaviors, the negative deviation was maximal for Tinuvin 326 and molecules including a BHT pattern. The introduction of a second substance increased the previous trend with an additional deviation $\left\langle \beta_{XY}^{all} \right\rangle_Y$ mostly negative [Fig. 7(c)]. The confusion matrix extended to quantifications [Fig. 7(d)] assessed the average amount, which should be related to the molecule read row-wise.

Deconvolution of theoretical complex mixtures

In practice, mixtures are expected to contain more than two unknown substances and a significant
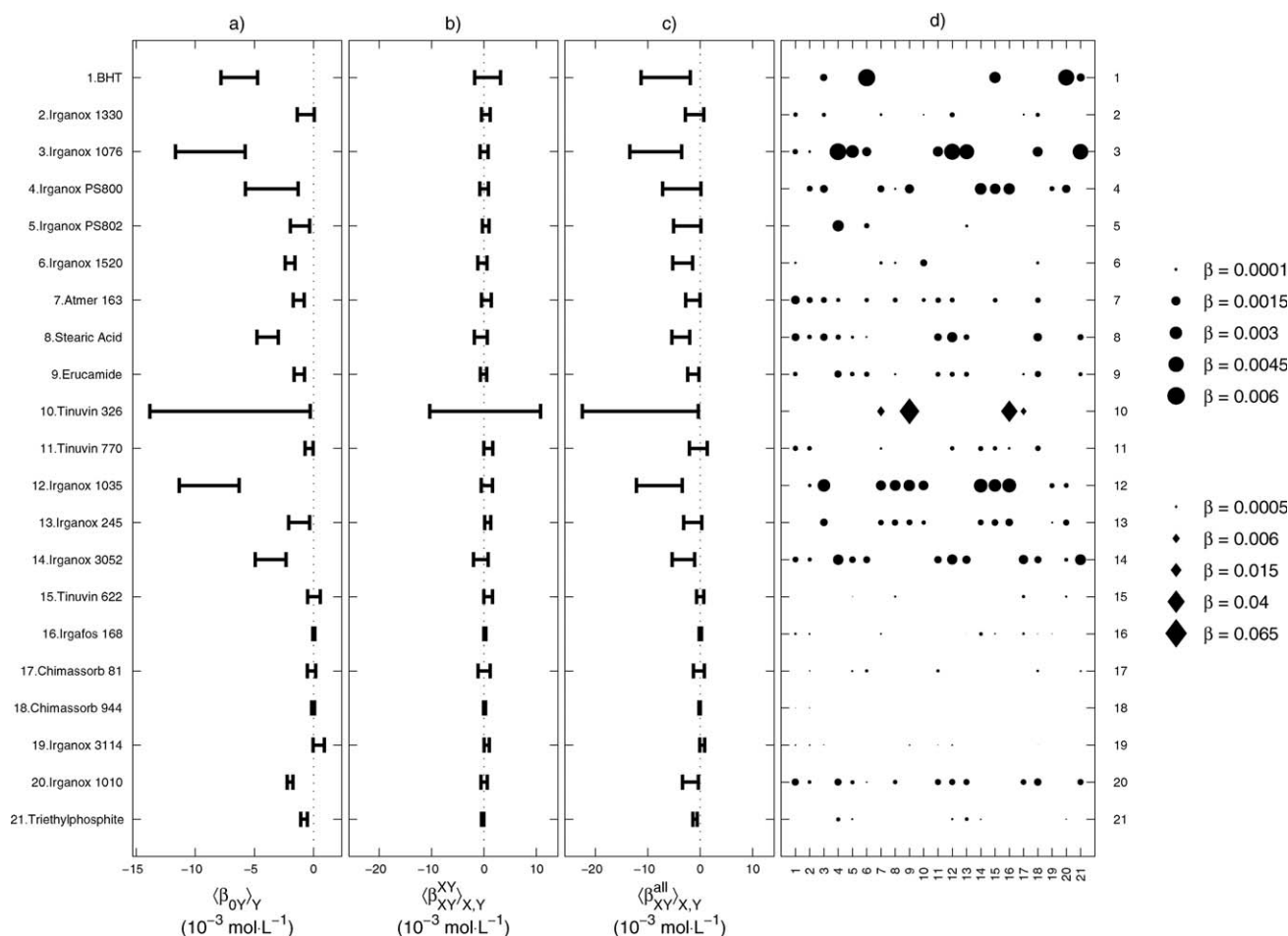
Figure 7 Quantification biases on Y concentration for binary mixtures $X + Y$ as defined in eq. (8): (a) biases associated to Y alone when no W was added, $\langle \beta_{0Y} \rangle_Y$; (b, c) average biases associated to increasing concentrations in X for all possible X; (d) biases associated to a specific substance X. Biases in b were calculated with dictionaries containing only molecules X and Y, whereas they were calculated with all 21 additives in a, c, and d.

amount of oligomers and other residues from the polymer, denoted PE. In addition, some substances can be missing in the dictionary. To assess the performance of the identification procedure defined by eq. (6), three typical situations were theoretically constructed from the individual spectrum of each substance:

- Extract A: five substances with low binary biases and PE; all substances are indexed in the dictionary;
- Extract B: three substances with significant binary biases and PE; all substances are indexed in the dictionary;
- Extract C: five substances and PE; three substances are not indexed in the dictionary (three columns are removed from Δ).

To match real extracts, the concentration in PE was set to contribute to 15% to the whole variance of the measured spectrum. The inversion procedure was applied on the synthesized spectra including 5% of white noise. To retrieve a reliable statistics on 5 and 95% percentiles, the whole process was reiterated 500 times. All determinations relied on a large dictionary, including 21 substance accessions, except for extract C where only 18 entries were considered, and including four generic chemical group accessions: C—S, C—N, C—O, and N—H. The corresponding identification and quantification results are plotted in Figure 8 as residues spectra and as expected concentrations for all possible molecules and chemical groups listed in the database. To help the identification of possible false assignation of substances, the molecules were ordered according to the overall distances between spectra as plotted in Figure 5(b). It is thus highlighted that a concentration attributed to a given substance could also be shared with molecules in the neighborhood (i.e., with a similar response). As molar concentrations were used, the mass balance between homologous molecules could be determined.
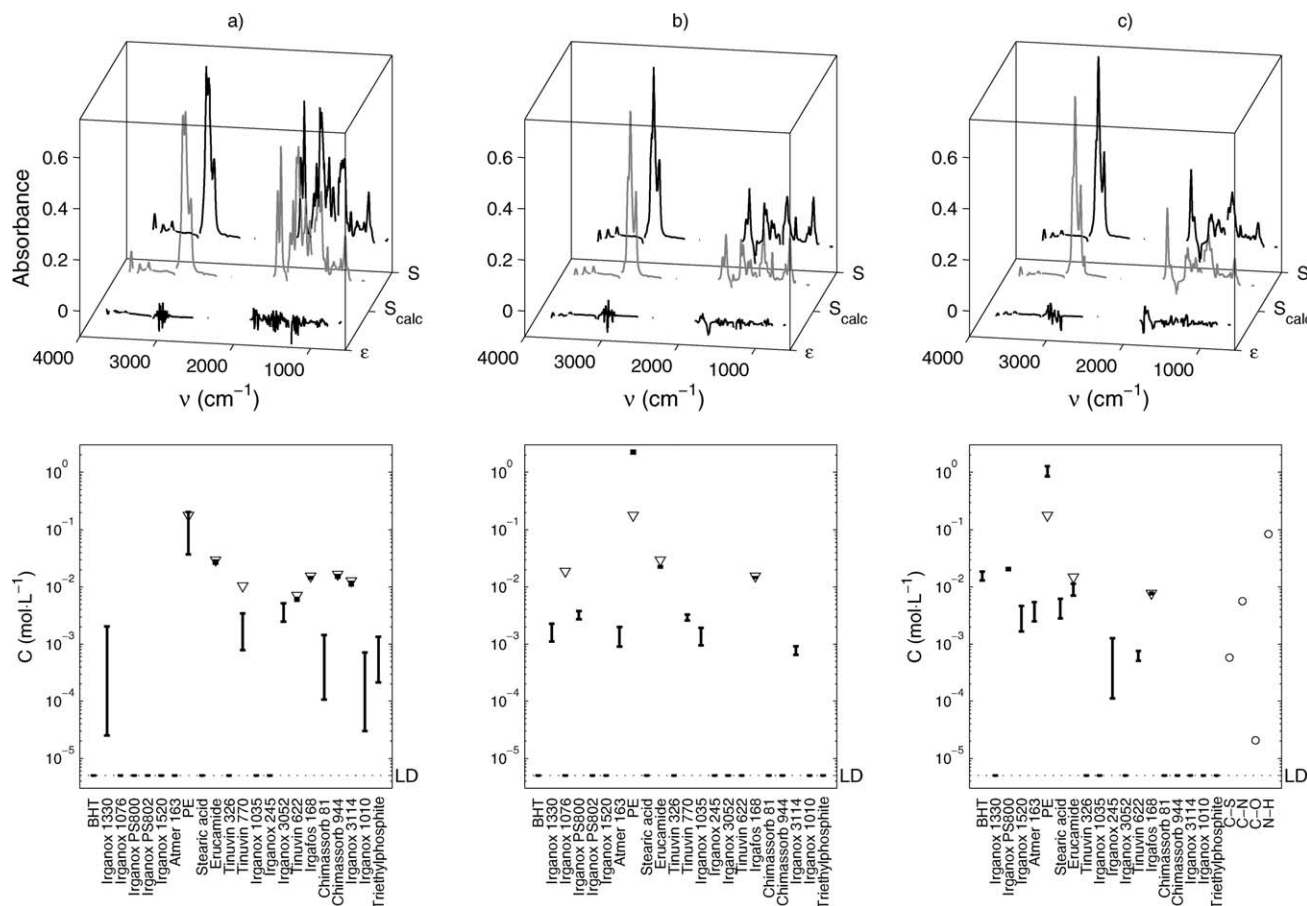
Figure 8 Identification and quantification capabilities on three typical synthesized mixtures including 5% white noise: (a) extract A, (b) extract B, and (c) extract C. Spectra include the synthesized spectrum, S, the calculated spectrum after identification, S_{calc}, and the residues, ε. Calculated concentrations in DCM are gathered as intervals for all listed species in the dictionary. Each interval represents the 95% confidence intervals based over 500 repetitions. Zeroed concentrations in the solution have signed value equal to the theoretical detection limit (DL). True concentrations appeared as open triangles. Chemical functions are reported only when their concentrations were determined non null.

In extract A, all molecules were well identified with predicted concentrations in good agreement with theoretical ones [Fig. 8(a)]. Because of the presence of some false positives, the concentrations tended to be underestimated. False positives were easily separated from real additives as their concentrations were one magnitude order much lower. In real processed materials, they would appear with concentrations much lower than those recommended by the industry. It is underlined that the solution remained mainly sparse, and that no additional functional group was introduced by the resolution algorithm. As they are subjected to different SMLs, the separation between primary antioxidants (Irganox 1076, Irganox 1010, and Irganox 3114), secondary antioxidants (Irgafos 168), and light stabilizer (Chimassorb 944) was particularly remarkable.

A similar behavior was observed in extract B [Fig. 8(b)]. Irganox 1076 was, however, not identified and was replaced by a false-positive Irganox PS800 with a very similar absorption spectrum (Fig. 4). The surface agent Atmer 163 tended to be mistaken for

polyethylene residues. Besides, as Irganox 1076 presented an aliphatic group similar to octodecane, it led to a significant overestimation of polyethylene residues contribution.

Mixture C was a complex case, where Irganox 1076, Irganox PS802, and Tinuvin 770 were present in the mixture with respective concentrations of 20, 7, and 10 mol L^{-1} but missing in the dictionary Δ. Under constraints of non-negativity, the total variance could not be explained by the listed substances alone, and four additional functions were additionally identified. Although its spectrum was unknown, Irganox 1076 was substituted in a consistent manner by BHT and Irganox PS800 with a very similar spectrum (Fig. 4). The introduction of C—S and N—H functions was a reliable signatures of molecules belonging to the family of Irganox PS802 and Tinuvin 770, respectively. As the spectra of such functions were idealized, they could not be used for quantification.

Examples follow-up drove some practical conclusions. Phosphorous acid esters such as Irgafos 168 were well identified and quantified. Chimassorb 944,
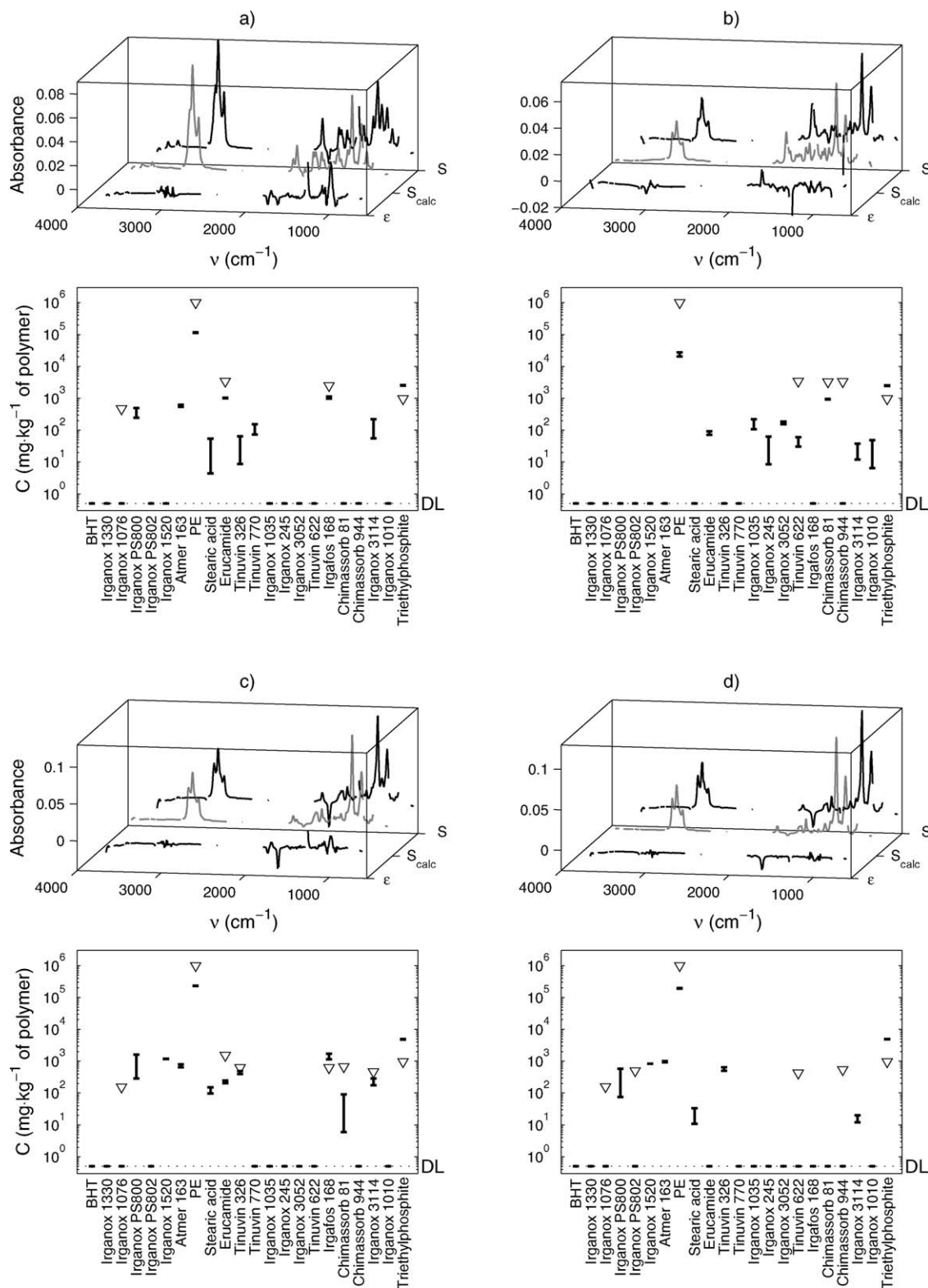
Figure 9 Identification and quantification capabilities on four real extracts from high-density polyethylene films: (a) PE1, (b) PE2, (c) PE3, and (d) PE4. The data are expressed as in Figure 8 except the concentrations are reported in the initial processed films instead of in the extracts. Concentrations measured on the same samples by a standard HPLC method appeared as open triangles.

Tinuvin 622, and Irganox 3114 were well quantified but subjected to false positive. Erucamide was identified but its concentration was underestimated. Irga-

nox 1076 was never identified, whatever it was present or not, and was systematically replaced by Irganox PS800. Removing Irganox PS800 from Δ

corrected the situation, but it was not a reliable choice on commercial samples. The overall approach was enough robust to propose additional functions where a compound in the mixture exhibited a spectrum sufficiently different from those recorded. The procedure can be easily enriched by the introduction of new substances.

Deconvolution of the extracts of real formulations

In the previous examples, the deconvolution was applied to mixtures where each compound was introduced with nominal concentrations. Within a real mixture, the deconvolution was complicated by a contribution to the total variance, which was highly inhomogeneous. To get a multiscale deconvolution procedure either on major and minor substances, the following two-pass deconvolution procedure was applied to four different real formulations of HDPE, denoted $\{PE_i\}_{i\ =\ 1..4}$:

1. application of normal weights, W, to all wavenumbers and identification;
2. reweighting W according to $1/|\varepsilon_v|$ from previous step and identification restricted to the nonfingerprint region (above 1500 cm^{-1});
3. reweighting W according to $1/|\varepsilon_v|$ from previous step and identification restricted to nitrogen-containing compounds between 1500 and 2500 cm^{-1} and beyond 3200 cm^{-1};
4. all previous steps were reiterated by starting from step 3 down to step 1.

The concentrations of minor compounds, which explained less than 20% of the total variance, were defined as the maximum of six determinations. The concentrations of other compounds were derived from step 1 alone to prevent additional biases due to nonlinear approximations of spectra deviations. The two-pass deconvolution in forward and reverse order with iterative reweighting ensured that details in the nonfingerprint region, which supports most of the variance, could be revealed without introducing a large numbers of false positive. The overall sparsity of the solution was controlled thanks to nonnegativity constraints applied to all steps. Spectra obtained at step 1 and final concentrations after the two-pass deconvolution are plotted in Figure 9. The concentration results are expressed in the usual manner for compliance testing in mg kg^{-1} of polymer (Table II). An arbitrary threshold of 0.1 mg kg^{-1} was applied to all unidentified substances. Confidence intervals were obtained by adding 5% white noise to the measured spectrum and by repeating the whole procedure 500 times. This protocol contributed via stochastic resonance to enhance the

response of the deconvolution procedure to small contributions.

Although the identification was not exact for all substances, the magnitude orders agreed well the real contents. False positives appeared at much lower concentrations (traces) or involved molecules with very close spectra and/or with close chemical structure. As a rule of thumb, most of false positive were reliably identified by large confidence intervals over about one magnitude order. Exceptions appeared for linear molecules easily confused with polymer residues such as Atmer 163 and for molecules including presenting several BHT patterns. Because of false positives, the concentrations of most identified substances were underestimated.

In details, PE1 had a composition close to the previous extract B and exhibited a very similar behavior. Irganox 1076 was replaced by Irganox PS800 and in a less extent by Tinuvin 770. Triethylphosphite and Erucamide were well identified. According to Figure 7(e), the underestimation would be caused by 1076, Erucamide and triethylphosphite. PE2 contained three light absorbers and two of them were detected. Chimassorb 81 was reliably detected, whereas Chimmassorb 944 was mistaken with antioxidants Irganox 3114 and Irganox 1010, whose responses are closely related as illustrated Figure 7(e). Similarly, the Tinuvin 622 contribution was partly replaced by an amount of Irganox 3052. PE3 and PE4 were very realistic formulations of polyethylene including primary antioxidants, secondary antioxidants, and light stabilizers. The method identified either the right substance or the immediately adjacent substances. The analyses were highly convincing in PE3, whereas they were more difficult to interpret in PE4. However, two substances or analogous ones were not identified in PE4: Chimassorb 944 and Tinuvin 622. As both additives are polymeric, they might be identified as smaller additives with similar chemical formula. Tinuvin 326 could thus replace Tinuvin 622. The last poorly identified substance, Erucamide, was replaced consistently by Atmer 163.

The ability of the whole approach to predict the lumped concentration of additives belonging to a same class of additives or chemical functions is presented in Figure 10. The corresponding estimated concentrations were cumulated by classes and plotted against their reference values in the four tested samples. On complex extracts, the proposed simplifications made it possible to merge reconstructions from substances with tangled spectra. The predictions were in well agreement for primary and secondary antioxidants, and ultraviolet light absorbers. Significant underestimation occurred only for surface modifiers.

TABLE II
Composition of Processed High-Density Polyethylene Films

Additive name	PE1 (mg kg^{-1})	PE2 (mg kg^{-1})	PE3 (mg kg^{-1})	PE4 (mg kg^{-1})
Irganox 1076	467 ± 23	–	156 ± 3	159 ± 27
Irgafos 168	2497 ± 167	–	626 ± 40	–
Erucamide	3436 ± 116	–	1523 ± 152	–
Chimassorb 81	–	3293 ± 370	668 ± 46	–
Chimassorb 944	–	3327 ± 237	–	545 ± 26
Tinuvin 622	–	3416 ± 960	–	427 ± 120
Irganox 3114	–	–	463 ± 42	–
Tinuvin 326	–	–	626 ± 61	–
Irganox PS 802	–	–	–	502 ± 17
Triethylphosphite[a]	969 ± 10	969 ± 10	969 ± 10	969 ± 10

[a] Substance added to the extract, with a concentration expressed as it was present in the processed film.

Separation of additives by their chemical functions

As tested phenolic antioxidants additives included a repeated BHT pattern and could be confused with other hindered molecules such as light stabilizer, their absolute identification was identified as a stiff mathematical problem. As a typical example, the ubiquitous Irganox 1076 was commonly mistaken with a less common antioxidant Irganox PS800. A possible strategy to identify robustly Irganox 1076 and to contribute to separate antioxidants between several alternatives was to obtain a signature of the two patterns characteristic of Irganox 1076: the BHT head and the complementary tail, consisting in an ester function and an octadecane block. Because PS800 does not include any BHT pattern, the presence of Irganox 1076 could be estimated very likely as soon as the ratio between the number of BHT head pattern and the number of tail pattern would be significantly greater than 0. On the opposite, a value closer to unity would reveal the presence of a significant amount of hindered phenolic antioxidants comprising several BHT patterns. By contrast, values greater than 1 were very unlikely as the signature of the tail was common several additives. The signature of the tail in Irganox 1076 was retrieved by subtracting the BHT contribution from the molar spectrum of Irganox 1076. Optimal wavenumbers weighting for each pattern were derived by studying the linearity of the spectrum with concentration. The molar concentration ratios inferred from specific deconvolutions of previous extracts are summarized in Figure 11. The exact ratio, which accounted all linear molecules, is also plotted for comparison.

Although the ratio did not sign any substance, it supported unambiguously that PE2 did not contain any phenolic antioxidant and that the composition in phenolic antioxidants in PE3 was significantly different from PE1 and PE4 with a likely presence of an antioxidant consisting of several BHT patterns. It confirmed thus the presence of Irganox 3114 including three BHT patterns in PE3 [Fig. 9(c)]. By contrast, the lower ratio in PE4 confirmed the presence of a significant amount of aliphatic thioethers, identified as Irganox PS802 [Fig. 9(d)]. The predictions of this ratio were highly reliable and provided an additional framework to choose between several alternatives.

Other ratios were found to be valuable to improve predictions presented in Figure 9 at least qualitatively. Table III presents the relative concentrations in some specific patterns as they were identified. Among them, the acid pattern found in PE1 was related to stearic acid, which was poorly identified with the global procedure. The piperidinyl group typical of Tinuvin 770, Tinuvin 622, and Chimassorb 944 was accurately detected in PE2 and PE4, whereas none of them were initially detected. Other patterns such as the ester function and ring patterns in Irganox 1330 and 3114 were not identified, as they were either not accurately calibrated by successive subtractions of spectra or not supported by a significant variance in the measured spectra.

CONCLUSIONS

A semisupervised deconvolution procedure of FTIR spectra based on a ridge regression procedure has been described to identify and quantify the concentrations of plastics additives in polymer extracts. The methodology was designed to work obtained on complex mixtures including several compounds with either known or unknown compounds. The proposed formulation offered a consistent weighting procedure to derive sparse solutions focused either on substances, chemical functions, or a combination of both. This strategy was particularly suited to additives including repeated patterns. The automatic switch between a global and a local solution was performed using an iteratively reweighted least square criterion, which zoomed either in or out on unexplained spectra residues. As the added non-negativity constraints acted
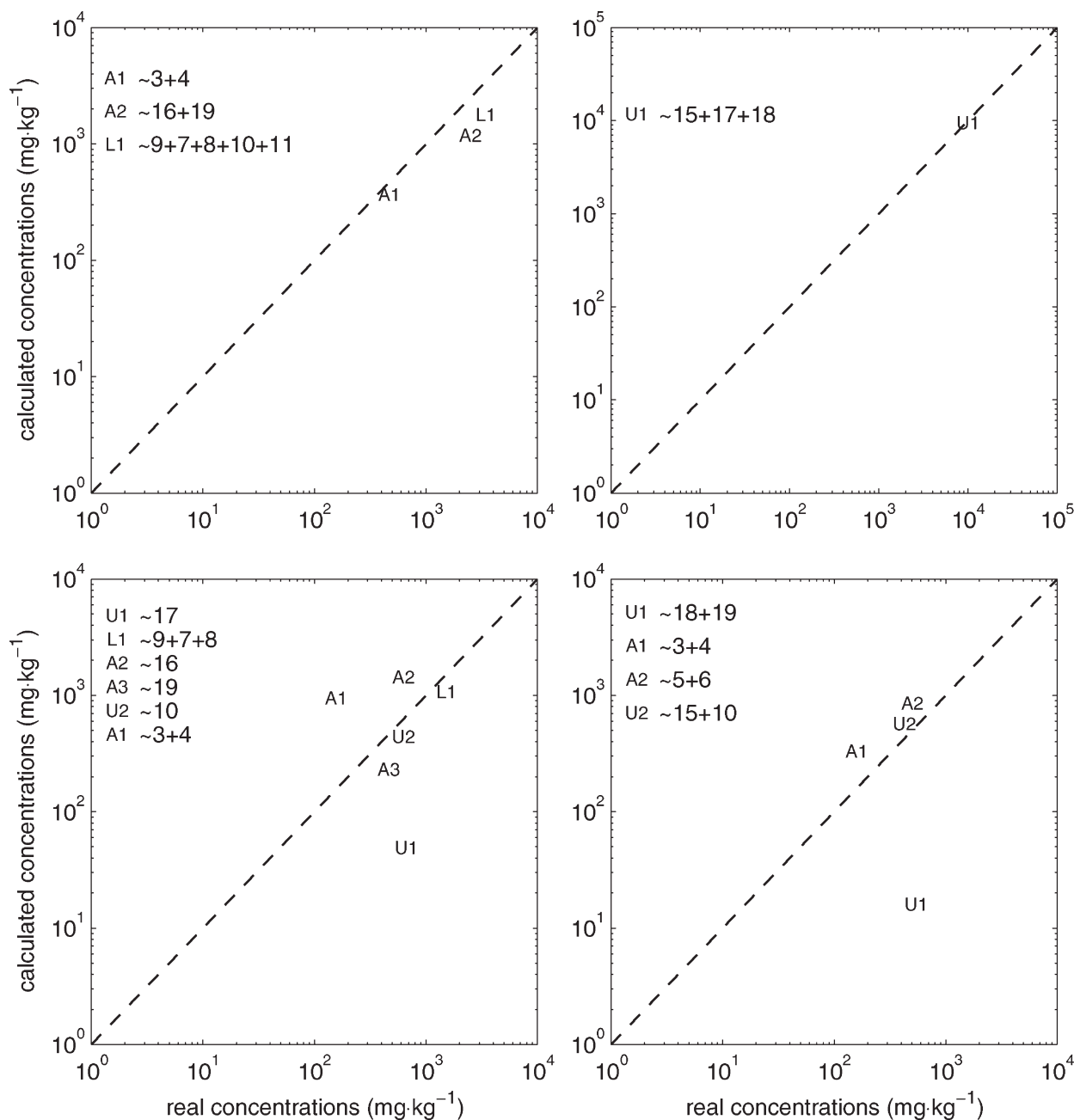
Figure 10 Mass balance in substances with similar technological functions against the theoretical extent in processed films: (a) PE1, (b) PE2, (c) PE3, and (d) PE4 plotted in Figure 9.

as a Wiener filter, they avoided false positives while imposing a detection threshold to small contributions involving 1% or less of the total variance in the measured spectrum. This inherent limitation was partly overridden by invoking systematically stochastic resonance effects via Monte-Carlo sampling. Adding randomly a white noise to the measured spectrum caused low signal intensities to cross more often the identification threshold and offered statistics to our nonlinear identification technique.

The whole technique has been implemented within a specific Matlab toolbox (Mathworks, USA), so-called ACTIA-LNE, and calibrated on 21 common additives of polyolefins and four chemical functions typical of possible nonlisted substances. As the calibration method took into account the linearity and detection limit of the spectrophotometer as well as interactions with the extraction solvent, the generated dictionary of spectra and related optimal weights depended on the experimental device and appeared consequently more reliable than commercially available FTIR spectra databases. However, although the deconvolution method has been applied to extracts in DCM, it could be directly applied to processed films in transmission mode or in attenuated total reflectance subsequently to an
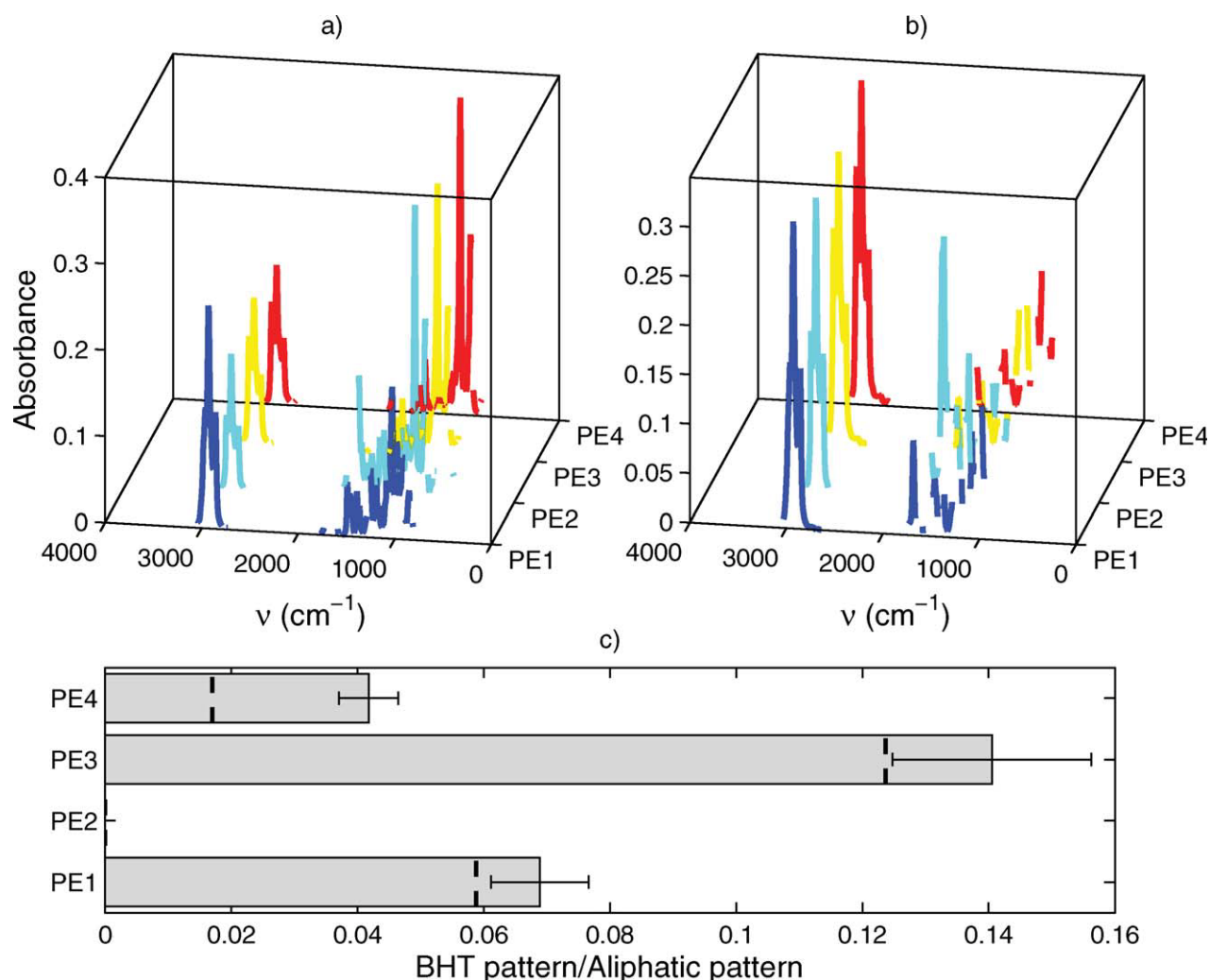
Figure 11 Absorption spectra of extracts of processed films by considering: (a) nominal weights for the BHT pattern, (b) nominal weights for an aliphatic pattern similar to the Irganox 1076 tail; ratio of concentrations between previous patterns. [Color figure can be viewed in the online issue, which is available at wileyonlinelibrary.com.]

appropriate calibration. This approach, which involves a higher contribution of the background and a lesser sensitivity to trace additives, is currently under validation in 2D FTIR mode (by changing temperature). In tested extracts, the background was both related to the intense bands of DCM and to polymer residues (oligomers mainly). As the polymer background could not be known *a priori*, three commercial virgin flakes of high-density polyethylene were used to assign a normalized spectrum to polymer residues. The theoretical concentration associated to these residues was therefore an additional unknown in the inversion problem.

The ill-posedness of the general deconvolution problem was assessed by calculating the distances between spectra, the identification and quantification biases for all possible binary mixtures. A table of confusion was generated to support the interpretation of false positives, masking effects, and possible sources of underestimations. The whole procedure was applied to four

theoretical and four real mixtures including up to eight compounds. In all cases, the method provided valuable conclusions by either identifying the right substances or substances which were chemically close. The determination of the lumped concentration of substances belonging to a same class of additives (antioxidants, light stabilizers, and surface agents) was as reliable as

TABLE III
Predicted Relative Concentrations in Specific Pattern in Processed Samples

Pattern	PE1	PE2	PE3	PE4
BHT	1 (1)	0 (0)	1 (1)	1 (1)
Ester function	0 (1)	0 (0)	0 (0)	0 (6)
Ring in Irganox 1330	0 (0)	0 (0)	0 (0)	0 (0)
Ring in Irganox 3114	0 (0)	0.01 (0)	0 (0.33)	0 (0)
Aliphatic function	15 (17)	1 (1)	7 (8)	24 (59)
Ring in Irganox 770	0 (0)	0.21 (0)	0 (0)	0 (0)
Acid function	0.01 (0)	0 (0)	0 (0)	0 (0)

Real concentrations are expressed in brackets.

1514 GILLET, VITRAC, AND DESOBRY

techniques involving a physical separation such as chromatographic techniques. In real conditions, the "absolute" identification of additives was possible only for some substances. Appropriate identification and quantification were revealed after adding random noise to measured spectra by low confidence intervals on concentration estimates. When substances were ranked according to the closeness of their FTIR responses (i.e., linkage criteria), reliable identification but possibly poor quantification was recognized by large confidence intervals but low overlapping rate between close substances. Poorly identified or quantified analysis required an additional interpretation of spectra based on specific chemical functions.

Although some fuzziness may remain after deconvolution, the identification of possible migrants and of their amounts in a packaging material is of prime importance to start an assessment of its compliance with EU regulations. Indeed for most additives and contact applications, abacuses or software are available to calculate the maximum amount in the polymer, which could permit to demonstrate the compliance with mathematical modeling.[7] Because of inherent uncertainty in physicochemical properties, these approaches do not claim to predict the real migration rate but an overestimate instead with sufficient safety margin. As a result, the subsequent steps should focus only on situations (substances and concentrations) for which the compliance could not be demonstrated with the previous approach. Next steps might include a discussion with the provider or complementary measurements with conventional techniques.[22] A companion work aims at integrating databases, simulation tools, and fast identification by FTIR methods to design automated decision tools to assist enforcement and control laboratories in identifying noncompliant plastics materials intended to be in contact with food. As a rule of thumb and in case of doubt on the real substance, an additive including n subunits can be always replaced by a migrant consisting in a single unit at a concentration n times higher. The question for compliance testing is then: "which value of n could demonstrate the compliance?" When the calculated n is suspected to be too small, a validation by or with the provider is required.

As the methodology was proven to be quantitative at least for lumped additives, it might also be envisioned to monitor desorption rates during standard migration tests.

NOMENCLATURE

Roman symbols

A_i	substance used as additive
C	molar concentration (mol L^{-1})

C	concentration vector
D	dictionary matrix of known substances
DCM	dichloromethane
i	index
I	identity matrix
j	index
PM	polymer and related residues
r	correlation coefficient
S	measured spectrum (absorbance)
S	measured spectrum vector
U_j	unidentified substance (not belonging to the dictionary)
X	arbitrary substance
Y	arbitrary substance
W	weight matrix

Greek symbols

α	molar extinction coefficient of the considered cuvette (L mol^{-1})
β	concentration bias (mol L^{-1})
γ	molar concentration in unknown substance (mol L^{-1})
ε	model error (absorbance)
$\boldsymbol{\varepsilon}$	error vector
$\bar{\Delta}$	weighted dictionary matrix of known substances
$\Delta_\mathbf{r}$	weighted dictionary matrix of unknown substances
λ	wave length
ξ	regularization coefficient in eq. (6)
Σ	effective spectrum (absorbance)
ω	wavenumber

Special operators

diag(**X**)	main diagonal of matrix **X**
$<X>$	ensemble average of X
$\mathbf{X}^T$	transpose of **X**
var(**X,Y**)	variance of **X** respectively to weights **Y**

References

1. European Commission. Official J Eur Union 2002, L220, 18.
2. European Commission. Official J Eur Union 2004, L338, 4.
3. European Commission. Substances listed in EU directives on plastics in contact with food. Available at: http://ec.europa.eu/food/food/chemicalsafety/foodcontact/eu_substances_en.pdf, Accessed September 2008.
4. European Commission. Official J Eur Union 2007, L97, 50.
5. European Commission. Official J Eur Union 2007, L384, 75.
6. Vitrac, O.; Hayert, M. AIChE J 2005, 51, 1080.

7. Vitrac, O.; Hayert, M. In New Trends Chemical Engineering Research; Berton, L. P., Ed.; Nova Science: New York, 2007; pp 251–292.

8. Feigenbaum, A.; Scholler, D.; Bouquant, J.; Brigot, G.; Ferrier, D.; Franz, R.; Lillemark, L.; Riquet, A. M.; Petersen, J. H.; Van Lierop, B.; Yagoubi, N. Food Addit Contam 2002, 19, 184.

9. Bart, J. C. J.Additives in Polymers: Industrial Analysis and Applications; Wiley: Chichester, 2005.

10. Choller, D.; Vergnaud, J. M.; Bouquant, J.; Vergallen, H.; Feigenbaum, A. Packag Technol Sci 2003, 16, 209.

11. Bart, J. C. J.Plastics Additives: Advanced Industrial Analysis; Ios Pr Inc.: Amsterdam, 2006.

12. Hummel, D. O.Atlas of Plastics Additives: Analysis by Spectroscopic Methods; Springer-Verlag: Berlin, 2002.

13. Vigerust, B.; Kolset, K.; Nordenson, S.; Henriksen, A.; Kleveland, K. Appl Spectrosc 1991, 45, 173.

14. Allen, N. S.; Palmer, S. J.; Marshall, G. P.; Gardette, J. L. Polym Degrad Stab 1997, 56, 265.

15. Zehnacker, S.; Marcha, J. Polym Degrad Stab 1994, 45, 435.

16. Möller, K.; Gevert, T.; et Holmström, A. Polym Degrad Stab 2001, 73, 69.

17. Földes, E.; Maloschik, E.; Kriston, I.; Staniek, P.; Putanszky, B. Polym Degrad Stab 2006, 91, 479.

18. Yagoubi, N.; Denuzière, A.; Pellerin, F.; Ferrier, D. Ann Phar Fr 1996, 54, 126.

19. Vitali, M. Polym Test 2001, 20, 741.

20. Silverterin, R. M.; Webster, F. X.; Kiemle, D. J.Spectrometric Identification of Organic Compounds, 7th ed.; Wiley: New York, 2005.

21. Murphy, J.Additives for Plastics Handbook, 2nd ed.; Elsevier: Oxford, 2003.

22. Gillet, G.; Vitrac, O.; Tissier, D.; Saillard, P.; Desobry, S. Food Addit Contam 2009, 26, 1556.

23. Bagnati, R.; Blanchi, G.; Marangin, E.; Zuccato, E.; Fanelli, R.; Davoli, E. Rapid Commun Mass Spectrom 2007, 21, 1998.

24. Sun, C.; Chan, S. H.; Lu, D.; Lee, H. M. W.; Bloodworth, B. C. J Chromatogr A 2007, 1143, 162.

25. Adams, M. J.Chemiometrics in Analytical Spectroscopy, 2nd ed.; The Royal Society of Chemistry: Cambridge, 2004.

26. Tikhonov, A. N.; Arsenin, V.Solution of Ill-Posed Problems; Wiley: New York, 1977.

27. Hansen, C. Numer Algorithms 1994, 6, 1.

28. Coleman, T. F.; Li, Y. SIAM J Optim 1996, 6, 1040.

29. Garrido-López, Á.; Tena, M. T. J Chromatogr A 2005, 1099, 75.

30. Stuart, B.Infrared Spectroscopy: Fundamentals and Applications; Wiley: Hoboken, 2004.